Title
Sequential primed kinases create a damage-responsive phosphodegron on Eco1

Permalink
https://escholarship.org/uc/item/0kp430gg

Journal
Nature Structural & Molecular Biology, 20(2)

ISSN
1545-9993

Authors
Lyons, Nicholas A
Fonslow, Bryan R
Diedrich, Jolene K
et al.

Publication Date
2013-02-01

DOI
10.1038/nsmb.2478

Peer reviewed

Sequential Primed Kinases Create a Damage-Responsive Phosphodegron on Eco1

Nicholas A. Lyons[1], **Bryan R. Fonslow**[2], **Jolene K. Diedrich**[2], **John R. Yates III**[2], and **David O. Morgan**[1]

[1]Department of Physiology, University of California, San Francisco, 600 16th St., San Francisco, CA 94158

[2]Department of Chemical Physiology, The Scripps Research Institute, 10550 N. Torrey Pines Rd., La Jolla, CA 92037

Abstract

Sister-chromatid cohesion is established during S phase when Eco1 acetylates cohesin. In budding yeast, Eco1 activity falls after S phase due to Cdk1-dependent phosphorylation, which triggers ubiquitination by SCF-Cdc4. We show here that Eco1 degradation requires the sequential actions of Cdk1 and two additional kinases, Cdc7–Dbf4 and the GSK-3 homolog Mck1. These kinases recognize motifs primed by previous phosphorylation, resulting in an ordered sequence of three phosphorylation events on Eco1. Only the latter two phosphorylation sites are spaced correctly to bind Cdc4, resulting in strict discrimination between phosphates added by Cdk1 and Cdc7. Inhibition of Cdc7 by the DNA damage response prevents Eco1 destruction, allowing establishment of cohesion after S phase. This elaborate regulatory system, involving three independent kinases and stringent substrate selection by a ubiquitin ligase, enables robust control of cohesion establishment during normal growth and following stress.

INTRODUCTION

Protein kinases and ubiquitin ligases are key regulators of the cell division cycle. The Cyclin-Dependent Kinases (Cdks) are particularly important, phosphorylating hundreds of substrates involved in numerous cellular processes[1,2]. Cdk function is linked to another important regulatory mechanism, protein degradation, by the Skp1–Cullin–F-box (SCF) ubiquitin ligase[3]. The F-box subunit of SCF recruits substrates by interacting with specific sequence motifs (degrons), which often contain phosphorylation sites. Phosphodegrons created by Cdks and other kinases tie SCF to many important cell cycle processes. In yeast, for example, phosphorylation of several cell-cycle regulators by Cdk1 leads to their

recognition by the F-box protein Cdc4 (Supplementary Table 1). The vertebrate Cdc4 ortholog, Fbw7, also targets many phosphoproteins involved in cell proliferation and tumorigenesis[4].

The preferred phosphodegron for Cdc4 and Fbw7 has been studied in considerable detail. Key insights came from phosphopeptide binding experiments, which showed that Cdc4 prefers peptides containing a phospho-serine or -threonine followed by a proline and preceded by hydrophobic residues: I/L-P-I/L-pS/pT-P-⟨RKY⟩₄ (where ⟨x⟩ refers to disfavored residues)[5]. This consensus overlaps with the consensus motif of Cdk1 (S/T*-P-x-K/R, where S/T* indicates the phosphorylated residue and K/R enhances affinity). It was subsequently found that Cdc4 has a higher affinity for peptides containing two phosphorylated sites[6], and that local sequence context is less critical than diphosphorylation[7]. SCF dimerization might also enhance binding of a multiply phosphorylated substrate[8], thereby increasing the processivity of ubiquitination[9].

Among its many cell cycle functions, SCF-Cdc4 helps regulate the generation of cohesion between sister chromatids as they are synthesized during S phase[10]. Sister-chromatid cohesion is established during S phase when the conserved protein Eco1 (also known as Ctf7) acetylates the Smc3 subunit of cohesin (refs. 11–14). Eco1 levels drop after S phase due to an increased degradation rate that requires Cdc4 and Cdk1 phosphorylation sites in Eco1, suggesting that phosphorylation of Eco1 by Cdk1 results in the generation of phosphodegrons that interact with Cdc4 (ref. 10). The drop in Eco1 abundance prevents cohesion establishment after S phase. Cdk1 and Cdc4 therefore collaborate to regulate chromosome segregation by preventing excess chromatid cohesion.

Cohesion establishment can also occur after S phase in cells with DNA damage[15–17], enabling efficient DNA repair[18]. DNA damage leads to phosphorylation of the cohesin subunit Scc1 (also called Mcd1) by Chk1 (ref. 19), which is thought to promote Scc1 acetylation at Lys84 and Lys 210 by Eco1 (ref. 20). The reactivation of cohesion establishment by DNA damage might also depend on the stabilization of Eco1 (ref. 10).

We set out to understand the mechanisms by which phosphorylation promotes the degradation of Eco1. We found that Eco1 degradation depends on a remarkable cascade of phosphorylation events involving Cdk1 and two additional kinases, Cdc7 and Mck1. We find that after priming by Cdk1 at one site, Cdc7 and Mck1 sequentially phosphorylate adjacent sites to create a diphosphodegron with high affinity for Cdc4, leading to degradation. We further show that Cdc7 inhibition upon DNA damage stabilizes Eco1, thereby reactivating cohesion establishment. Our experiments highlight the complex regulatory possibilities that can be achieved by multisite phosphorylation of key regulatory proteins.

RESULTS

Eco1 degradation depends on multiple kinases

Eco1 contains four potential Cdk1 phosphorylation sites in a region of predicted disorder (Fig. 1a). We showed previously that mutation of all four sites fully stabilized Eco1 (ref.

10). Here, we constructed Eco1 mutants lacking single phosphorylation sites and measured their degradation rates in metaphase-arrested cells treated with the translational inhibitor cycloheximide. We found that the central two sites (Thr94 and Ser99) are each necessary for Eco1 degradation (Fig. 1b). Mutation of Ser105 had little effect, while mutation of Ser67 promoted turnover (perhaps due to disruption of the nearby zinc finger).

Eco1 displays a mobility shift on gels supplemented with a phosphate-binding reagent[10,21]. Mutation of Ser99 abolished the mobility shift, suggesting that Ser99 phosphorylation is responsible for the shift (Fig. 1c). We showed previously that this shift occurs early in S phase, long before Eco1 is degraded, and also following DNA damage, when Eco1 is stabilized[10]. Thus, phosphorylation at Ser99 alone is not sufficient for Eco1 degradation.

Ser99 matches the full Cdk1 consensus sequence (S/T*-P-x-K/R), whereas Ser67, Thr94, and Ser105 are only minimal matches (S/T*-P). To assess Cdk1 activity toward these sites, we carried out kinase reactions *in vitro* with purified cyclin–Cdk1. Surprisingly, we found that the S99A mutation blocked all phosphate incorporation by Clb2–Cdk1, to the same degree as mutation of all four sites (Fig. 1d). Similar results were obtained with Cln2–Cdk1, Clb3–Cdk1, and Clb5–Cdk1, suggesting that Ser99 is the only efficient site for phosphorylation *in vitro* by most, if not all, forms of Cdk1 (data not shown).

To obtain an unbiased understanding of Eco1 phosphorylation, we identified sites of phosphorylation *in vivo* by mass spectrometry, using Eco1-Flag$_3$His$_6$ purified from yeast cells in which *CDC4* was transcriptionally repressed. We identified peptides phosphorylated at Thr94 and Ser99, as well as peptides with phosphates on Thr94 and the non-Cdk1 site Ser98 (Fig. 2a, b; Supplementary Fig. 1). Two other non-Cdk1 sites, Ser89 and Thr90, were also identified. Mutation of these residues had little (T90A) or no effect (S89A) on Eco1 stability (data not shown), so we focused our efforts on the other non-Cdk1 site, Ser98.

Ser98 is the first serine in an SSP motif, which is found at both the third and fourth Cdk1 consensus sites (Ser99 and Ser105). Mutation of both upstream serines (S98A S104A) fully stabilized Eco1 (Fig. 2c). Stabilization was not due to impaired Cdk1 activity toward Ser99, as Eco1 S98A S104A still displayed a mobility shift *in vivo* (Fig. 2d) and was phosphorylated by Cdk1 *in vitro* (Fig. 1d). Single mutations demonstrated that Ser98 phosphorylation is particularly important for Eco1 degradation, although Ser104 might also contribute (Fig. 2c).

In summary, Eco1 degradation depends primarily on phosphorylation at Thr94, Ser98, and Ser99. Only Ser99 is phosphorylated by Cdk1 *in vitro*, raising the possibility that other protein kinases modify the other two sites.

Cdc7–Dbf4 and GSK-3 are required for Eco1 degradation

The protein kinase Cdc7–Dbf4 is known to phosphorylate the first serine in SSP motifs that are phosphorylated at the second serine[22–25]. Cdc7 was therefore an appealing candidate for the kinase that phosphorylates Ser98 in Eco1.

Cdc7–Dbf4 is analogous to Cdk1–cyclin, as the catalytic subunit Cdc7 is active only when bound to Dbf4. Cdc7–Dbf4 is also called Dbf4-Dependent Kinase (DDK). Like those of Cdk1, Cdc7 levels are constant through the cell cycle, whereas Dbf4 oscillates, rising in late G1 and declining in mitosis[26,27]. DDK is required for the firing of replication origins, where its target is the Mcm replicative helicase[28]. It also has functions in mitosis[27] and meiosis[29].

DDK is essential for viability but can be deleted in the background of the suppressor mutation *MCM5-P83L* (ref. 30). To assess the role of DDK in Eco1 turnover, we measured Eco1 degradation in *dbf4 MCM5-P83L* cells arrested in metaphase. Deletion of *DBF4* resulted in full stabilization of Eco1 (Fig. 3a). Thus, both Cdk1 and DDK are necessary, and neither is sufficient, for Eco1 destruction.

As Thr94 is a poor Cdk1 site *in vitro* (Fig. 1d), we pursued the possibility that another protein kinase acts at this site. Interestingly, phosphorylation of Ser98 by DDK is predicted to create a consensus priming site for GSK-3 (glycogen synthase kinase-3), which phosphorylates amino acids four residues upstream of a previously phosphorylated residue (consensus motif: S/T*–x–x–x–pS/pT, where "x" is often proline)[31,32]. GSK-3 family kinases are the only kinases in yeast primed by +4 phosphorylation[24]. Furthermore, multiple substrates of vertebrate SCF-Fbw7 contain diphosphodegrons in which one site is phosphorylated by GSK-3 after priming of another site at the +4 position[4,33].

Among the four GSK-3 homologs of *S. cerevisiae*, Mck1 has been linked to the broadest range of functions[34]. Intriguingly, it has been implicated in the degradation of three SCF-Cdc4 substrates: Hsl1 (ref. 35), Rcn1 (ref. 36), and Cdc6 (ref. 37).

We analyzed Eco1 turnover in metaphase-arrested cells individually deleted for each GSK-3 homolog. Strikingly, Eco1 was stabilized in a *mck1* strain to the same extent as the Eco1-T94A mutant (Fig. 3b). Deletions of other GSK-3 paralogs had no effect, revealing a high degree of specificity among the GSK-3 family members.

Phosphorylated Eco1 is a direct target of Cdc7 and Mck1

Our results suggest that phosphorylation of Ser99 by Cdk1 primes Eco1 for phosphorylation at Ser98 by Cdc7, which then primes the protein for phosphorylation at Thr94 by Mck1. We tested this model directly by measuring kinase activities toward Eco1 peptides carrying phosphates at the predicted priming sites. Synthetic phosphopeptides (containing residues 91–103 of Eco1) were used instead of full-length Eco1 to ensure complete phosphorylation of priming sites.

Clb2-Cdk1 efficiently phosphorylated an unmodified peptide but not a peptide with phosphate at Ser99 (Fig. 3c), consistent with our other evidence that Ser99 is the sole major Cdk1 site. Interestingly, a phosphate on Ser98 also blocked Cdk1 activity. As mutation of Ser99 prevents all Cdk1 activity toward Eco1 (Fig. 1d), we suspect that Ser98 phosphorylation interferes with phosphorylation at Ser99.

DDK had no activity toward unmodified peptide, but rapidly phosphorylated the peptide with a phosphate at Ser99 (Fig. 3c). Phosphorylation was blocked by an alanine at position

98, but not at position 94, consistent with our priming hypothesis. Similarly, Mck1 phosphorylated an Eco1 peptide only if it contained a phosphate at Ser98, and only if it contained Thr94 (Fig. 3c). These data strongly support our model for the ordered phosphorylation of Eco1 by the three kinases.

Phosphorylation of Thr94 and Ser98 promotes Cdc4 binding

We next investigated the contribution of each phosphate in Eco1 to recognition by the Cdc4 subunit of SCF. Cdc4 displays a preference for diphosphorylated degrons, often grouped in clusters[6,7,38,39]. In those substrates with defined diphosphodegrons, phosphorylated residues are 2 or 3 residues apart, not the 4 residues between Thr94 and Ser99 in Eco1 (see Supplementary Table 1). Similarly, targets of vertebrate Fbw7 contain phosphorylation sites 3 residues apart[4]. We therefore hypothesized that phosphorylation of Ser98 brings the phosphate to within the ideal range for Cdc4 binding. We tested this idea by measuring the binding of various phosphopeptides to recombinant Cdc4–Skp1 *in vitro*. Phosphopeptides were synthesized, tagged with a fluorescent molecule (FITC), and incubated with increasing concentrations of Cdc4. Fluorescence polarization was used to measure bound peptide.

A peptide with phosphates at all three sites ("94-98-99") bound Cdc4 with an equilibrium dissociation constant of 10.3 μM (Fig. 4a). Affinity was much lower in the absence of phosphate at Ser98, but not in the absence of phosphate at Ser99. We observed moderate binding of a peptide phosphorylated at Thr94 alone, likely because the sequence around Thr94 is similar to the consensus Cdc4 binding motif[5]. This binding seems insufficient to mediate degradation *in vivo*, however, as the S98A and S99A mutations completely stabilize Eco1, and monophosphorylation at Thr94 is unlikely to occur since Mck1 requires priming at Ser98. Single phosphates at Ser98 or Ser99 had no effect on binding to Cdc4. Thus, phosphorylated Thr94 is the primary binding site whose affinity is supplemented by phosphorylated Ser98, as seen in other Cdc4 substrates[6,7,40].

These results suggest that the distance between phosphates is critical for Cdc4 recognition, as suggested by alignment of known Cdc4 and Fbw7 degrons (Supplementary Table 1 and ref. 4). To systematically test the importance of phosphate spacing, we measured Cdc4 binding to peptides containing variations in the distance between phosphates (Fig. 4b). Insertion of isoleucine (which should not alter Cdc4 binding[5]) before Ser98, moving the DDK site to the position of the Cdk1 site (peptide "94-98+I98"), removed the effect of the second phosphate. Removing a residue between Thr94 and Ser98 (peptide "94-99 N97") made phosphorylation at Ser98 unnecessary. The slightly reduced binding of this peptide relative to "94-98" could be due to local sequence context. Thus, efficient Cdc4 binding requires a maximum of 3 residues between phosphates.

We next tested whether there is a minimum distance between phosphates. Removing Asn97 from a peptide with phosphate at Ser98 (peptide "94-98 N97") did not reduce high affinity binding (Fig. 4b). However, deleting both Leu96 and Asn97, leaving only one residue between phosphates (peptide "94-98 LN"), blocked the effect of the second phosphate. Therefore, Cdc4 binds with high affinity only to substrates with 2 or 3 residues between phosphates.

We also tested the importance of phosphate spacing *in vivo*. Our model predicted that moving the sites closer by one residue (Eco1 N97) should remove the requirement for DDK in Eco1 degradation. Indeed, Eco1 N97 was highly unstable in a *dbf4* strain (Fig. 5a), even when Ser98 was mutated (Fig. 5b). The extreme instability of this mutant suggests that the activity of Cdk1 and Mck1 towards Eco1 is higher than that of DDK. Consistent with this explanation, the small amount of Eco1 N97 protein did not display a mobility shift in metaphase-arrested cells (Supplementary Fig. 2). We suspect that phosphorylation of this mutant by Cdk1 results in immediate degradation, whereas Cdk1-phosphorylated wild-type Eco1 is more stable due to limited phosphorylation by DDK.

As expected, Eco1 N97 was highly stabilized in a *mck1* strain (Fig. 5c). Stabilization was not complete, perhaps indicating that deletion of Asn97 causes non-specific protein turnover. However, Eco1 N97 displays a robust mobility shift in *mck1* cells, indicating that it is still targeted by Cdk1 *in vivo* (Supplementary Fig. 2). Moreover, additional deletions in this region (see below) fully stabilized the protein.

Eco1 was fully stabilized by insertion of isoleucine upstream of Ser98 (Eco1+I98) or by deletion of Leu96 and Asn97 (Eco1 L96 N97) or all three intervening residues (Eco1 96-98) (Fig. 5d). These results are generally consistent with our peptide binding results *in vitro*, with the exception of the Eco1 L96 N97 protein, in which phosphorylation sites are spaced at the same distance as the "94-98 N97" peptide that bound well to Cdc4 (Fig. 4b). Stabilization of this mutant is not due to reduced Ser99 phosphorylation by Cdk1 (Supplementary Fig. 2). Instead, stabilization is likely due to lack of phosphorylation by Mck1, as removal of Leu96 and Asn97 disrupts the correct spacing of the GSK-3 recognition motif[32].

DDK determines the timing of Eco1 degradation

To further characterize the DDK-independent degradation of Eco1 N97 , we examined protein levels over the cell cycle. As seen previously[10], wild-type Eco1 accumulated during S phase, declined in mitosis, and reappeared after mitosis (Fig. 6a). In contrast, Eco1 N97 levels declined in late G1, 20 minutes earlier than wild-type Eco1 (Fig. 6b). Destruction of Eco1 N97 began at the time that wild-type Eco1 displayed the Ser99-dependent mobility shift, but the mobility of Eco1 N97 did not change over the entire cycle. Eco1 N97 accumulated as cyclin levels dropped in mitosis. Thus, Eco1 N97 levels were inversely related to the amount of Clb–Cdk1 activity, suggesting that Cdk1 activity determines the timing of Eco1 N97 turnover and that Mck1 activity may be constitutive throughout the cell cycle. These results also suggest that the normal timing of Eco1 destruction in late S phase is determined by changes in DDK activity toward Ser98.

Inhibition of Dbf4 stabilizes Eco1 upon DNA damage

Our studies of the Eco1 N97 mutant suggested that the requirement for DDK provides a mechanism to delay Eco1 degradation until late S phase. We also considered a second rationale for regulation by DDK, based on our previous observation that Eco1 is stabilized by DNA damage[10]: DDK activity is thought to be reduced in yeast cells following DNA damage[41,42] (although perhaps not towards all substrates[26,30,43]). DNA damage causes

extensive phosphorylation of Dbf4, probably by the kinase Rad53 (refs. 42,44,45). Mutations in Dbf4 that reduce phosphorylation by Rad53 lead to inappropriate firing of late replication origins following DNA damage, suggesting that Dbf4 phosphorylation inhibits DDK function[46,47].

To test if DDK inhibition prevents the degradation of Eco1 in a damage response, we used *dbf4-m25* cells carrying a mutant Dbf4 that lacks Rad53 phosphorylation sites and is therefore refractory to damage-dependent inhibition[46]. Activation of a DNA damage response with hydroxyurea (HU) led to Eco1 stabilization (Fig. 7a), as seen previously[10]. However, Eco1 was rapidly degraded in *dbf4-m25* cells treated with HU (Fig. 7a), similar to *mec1* cells that lack the damage response. Maintenance of DDK activity in damage is thus sufficient to destabilize Eco1, supporting the role of Cdc7 in Eco1 turnover and indicating that Cdk1 and Mck1 activities toward Eco1 are not affected by the damage response. Also consistent with our model, DNA damage failed to stabilize the Eco1 N97 protein, which does not require DDK activity for turnover (Fig. 7b).

Discovering the molecular basis of Eco1 stabilization upon DNA damage allowed us to test whether it is required to establish new cohesion after damage. We used a variation of a previous protocol to measure the generation of damage-induced cohesion in metaphase[17]. In this experiment, cells establish normal cohesion in S phase using an Scc1 cohesin subunit containing a TEV protease site. Cells are arrested in metaphase, followed by treatment with a DNA-damaging agent and induction of Scc1 lacking the TEV site. TEV protease is then expressed to remove cohesion established during S phase. Only the cohesin expressed during the damage response is left to hold the LacI-GFP-tagged sister chromatids together.

In this assay, wild-type cells fail to establish new cohesion and about 50% of the cells contain separated LacI-GFP foci. Activation of establishment lowers this to about 30% (refs. 10,15,17,19). As seen previously, we found that DNA damage induced new cohesion in wild-type cells (Fig. 7c). This effect depended on lysines 84 and 210 in Scc1, which are likely Eco1 acetylation sites[20]. Damage did not induce new cohesion in *dbf4-m25* cells, but this was rescued by mutation of the two DDK consensus sites in Eco1, Ser98 and Ser104 (Fig. 7c). Additionally, the DDK-independent Eco1 N97 protein did not establish new cohesion after damage. Thus, the reactivation of cohesion establishment upon DNA damage depends on the increased levels of Eco1 caused by reduced DDK activity.

DISCUSSION

We report the discovery of an intricate series of phosphorylation events that controls the generation of sister chromatid cohesion through the phosphorylation and ubiquitination of the cohesion-promoting enzyme Eco1 (Fig. 7d). Our data suggest that Cdk1-dependent phosphorylation of one Eco1 residue, Ser99, primes for phosphorylation at the adjacent site, Ser98, by the cell cycle-regulated kinase Cdc7–Dbf4 (DDK) in late S phase. This then promotes a third phosphorylation at Thr94 by the GSK-3 homolog Mck1. The result is a precisely spaced pair of phosphates at Ser98 and Thr94 that create an interaction site for the SCF ubiquitin ligase subunit Cdc4. Because Dbf4 is inhibited by the DNA damage response,

full Eco1 phosphorylation is blocked following DNA damage, leading to high Eco1 levels and establishment of new cohesion after S phase.

The participation of Cdc7 in Eco1 degradation adds another layer of regulation to cohesion establishment and permits differential regulation in different cellular states. Regulation by DDK would be inconsequential, however, without the rigorous substrate discrimination we observed for Cdc4 and Mck1. The ability of Cdc4 to distinguish a phosphate attached by DDK from an immediately adjacent phosphate added by Cdk1 is remarkable. Likewise, the strict spacing of the GSK-3 consensus sequence means that the distance between phosphates in GSK-3 targets matches the ideal spacing for Cdc4 binding[4]. These features of Eco1 regulation together impose a set of strict conditions necessary to shut off cohesion establishment, enabling establishment activity to be correctly timed in the cell cycle and responsive to environmental perturbations.

This modularity and convergence of inputs is a common theme in biological regulatory systems. Regulatory proteins that respond only in the presence of multiple upstream inputs are called coincidence detectors and operate as logical 'AND' statements. Eco1 degradation represents an unusual case of a triple 'AND' statement integrating at least three separate inputs. Changes in any one input—oscillations in Cdk1 activity during the cell cycle or DDK inhibition after DNA damage, for example—dramatically influence the output, Eco1 degradation, and the biological process it controls, cohesion establishment.

Critical to the integration of the three Eco1 inputs is our finding that tight Cdc4 binding requires two or three amino acids between phosphates (Fig. 4). In crystallographic structures of Cdc4 bound to phosphopeptides with three residues between phosphates, the anchor phosphothreonine binds the center of the WD40 domain and the C-terminal phosphoserine interacts with Arg443, Ser464, Thr465, and Arg485, near the edge of the domain[6,39]. The C-terminal end of the peptide in these structures forms a small loop, allowing the second phosphoserine to contact the above residues. It is reasonable to predict that a degron with only two residues between phosphates could interact with the same side chains in Cdc4, but perhaps without making a loop. A peptide with four residues separating phosphates, however, may not be able to make the necessary contortions to align the second phosphate, and a degron with only a single intervening residue is probably not long enough to allow simultaneous interaction with both phosphate-binding sites.

Diphosphorylated Eco1 peptides have an affinity for Cdc4 that is similar to that of Sic1 phosphopeptides but weaker than those of the high-affinity substrates Tec1 and Ash1 (Supplementary Table 1). This moderate affinity could represent a selected trait that prevents Eco1 levels from getting too low after S phase, allowing cohesion establishment to be more easily reactivated. Another possibility is that the peptides do not fully recapitulate all of the binding contacts of the full-length substrate. Upstream residues could make extended interactions with Cdc4, as suggested by recent studies of long peptides from Sic1 (ref. 39).

It is also possible that additional phosphorylation sites in Eco1 contribute to Cdc4 binding. These sites might include the second SSP motif (Ser104-Ser105), as suggested by the

slightly additive effect of the S98A and S104A mutations (Fig. 2c), or possibly the more N-terminal phosphates identified by mass spectrometry (Ser89 and Thr90). Mck1 may catalyze phosphorylation of Thr90, since Thr94 is at the correct priming distance and GSK-3 kinases are known to sequentially phosphorylate substrates by creating their own consensus sites[31,32]. Phosphates at Thr90 and Thr94 could create another Cdc4 degron like that in Ash1, which contains three phosphates that create two redundant overlapping Cdc4 binding sites[40]. Ser89 might be phosphorylated by DDK after priming at Thr90, but this likely does not affect Eco1 degradation. Ser104 is too far from Ser99 to constitute a diphosphodegron, but might bind to another molecule in a Cdc4 dimer, as suggested for the interaction of human Fbw7 with its substrate cyclin E (ref. 8).

Our observation that Cdk1 only phosphorylates Ser99 was unexpected, as it shows that some S/T-P sequences are not efficiently targeted by Cdk1, even when they appear accessible to another kinase. Since Cdk1 was unable to phosphorylate Thr94 even in a short peptide (Fig. 3c), this substrate discrimination could be due to the surrounding primary or secondary sequence, though the exact cause is unclear. Another surprising result from our peptide phosphorylation studies was that a phosphate at the -1 position blocked Cdk1 activity (Fig. 3c).

Our evidence suggests that the timing of Eco1 degradation in late S phase is determined by DDK (Fig. 6b). These results are puzzling because Cdc7 activity is thought to be determined solely by binding to Dbf4, which is present throughout S phase[26,30]. DDK activity toward Eco1 might be limited until after the kinase completes its critical functions in the firing of replication origins. Interestingly, overexpression of replication initiation factors, including Dbf4, causes late replication origins to fire earlier in S phase[48,49], suggesting that Dbf4 levels are limiting for origin firing in late S phase. We found, however, that overexpression of *DBF4* has little effect on the timing of Eco1 degradation (data not shown). Thus, DDK activity toward Eco1 appears to be restrained during S phase by some mechanism that is not simply dependent on limiting Dbf4 levels. Further studies of other DDK substrates will be required to determine the regulatory mechanism that controls the timing of DDK activity toward Eco1.

The adaptive value of GSK-3 involvement in Eco1 degradation is less clear than that of DDK, but its recognition of primed substrates enables it to serve as a sensor for the activity of other kinases. This prevents attachment of the anchor phosphate at Thr94 until DDK is active, preventing spurious low-level binding of Cdc4 to the Thr94 monophosphate. The requirement for Mck1 ensures that Eco1 binding to Cdc4 goes from zero ("99" and "98-99" peptides in Fig. 4) to maximal ("94-98-99" peptide) with no intermediate. The system would not have this property if Cdk1 phosphorylated Thr94. Additionally, Cdk1 phosphorylation of Thr94 might require a basic residue at the +3 position, which would weaken Cdc4 binding[5]. Given their mutually exclusive consensus motifs, it will be interesting to see how many of the anchor phosphates in Cdc4 degrons are attached by Cdk1. In contrast, the GSK-3 motif overlaps perfectly with that of Cdc4: both proteins prefer substrates with three residues between phosphorylation sites. Thus, GSK-3 is ideally suited to provide the N-terminal phosphate in a Cdc4 degron. Consistent with this idea, metazoan GSK-3 and SCF have many substrates in common[4,33].

Mck1 is responsive to various cellular stresses[34], all of which seem to increase Mck1 activity towards certain substrates, possibly via priming by stress-activated kinases. These stress response pathways may not impinge on cohesion regulation, however, since Mck1 activity does not seem to be limiting for Eco1 degradation (Fig. 6b). The activity profiles of yeast GSK-3 homologs have not been as well characterized as those of their metazoan counterparts, but there are likely to be differences since GSK-3 family members in other eukaryotes tend to be active in cellular resting states and inhibited by growth factors[31], whereas Mck1 may be constitutively active[37]. Discovery of conditions that inhibit Mck1 activity would reveal new circumstances in which Eco1 could be reactivated, possibly indicating that DNA damage may not be the only stressor to modulate chromatid cohesion.

The results described in this study underscore the utility of post-translational modifications in precisely coordinating essential cell biological processes. To create an exact duplicate of an entire cell, dozens of diverse events must be properly organized and executed faithfully every generation. Just as multicellular development requires an extremely well-orchestrated series of interdependent events, so too must the events of the cell division cycle be exquisitely coordinated. An elegant regulatory system has thus evolved to ensure the fidelity of cell reproduction, and central to this is the accurate segregation of the genetic material.

ONLINE METHODS

General Methods

Yeast strains are derivatives of the S288C strain BY4741 (see Supplementary Table 2 for a list of strains and plasmids). Genetic manipulations were performed using standard methods[50]. Cell cycle arrests were achieved using 15 μg/ml nocodazole, 15 μg/ml alpha-factor, 2 μM 4-nitroquinoline, or 200 mM hydroxyurea for 3 h at 30°C; all arrests were confirmed by flow cytometric analysis of DNA content. Budding index and binucleate formation were counted using cells fixed in 0.02% sodium azide and either light microscopy or epifluorescence after staining DNA with 1 μg/ml 4′,6-diamidino-2-phenylindole (DAPI). Protein degradation was analyzed using 100 μg/ml cycloheximide to inhibit protein synthesis, followed by cell lysis by bead beating in urea buffer (20 mM Tris-HCl pH 7.4, 7 M urea, 2 M thiourea, 4% CHAPS).

Western blotting

Primary antibodies were anti-myc (9E10, Covance, 1:1000 dilution), anti-PAP (P 1291, Sigma, 1:5000), and anti-Pgk1 (22C5D8, Invitrogen, 1:10,000). Secondary antibodies coupled to horseradish peroxidase from GE Healthcare were used at 1:10,000 dilution. To visualize Eco1-Ser99 phosphorylation, the resolving portions of SDS-polyacrylamide gels were supplemented with 10 μM Phos-tag reagent[21] made using standard chemical techniques, 50 μM $MnCl_2$, and two-fold excess ammonium persulfate and TEMED.

Mass Spectrometry

Eco1-$Flag_3His_6$ was purified from P_{GALS}-HA3-CDC4 sic1Δ yeast cells grown overnight in 2% galactose, followed by dilution into 0.033% galactose. Following another day of growth, *CDC4* expression was repressed by addition of 2% dextrose for 3.5 h at 30°C and 4°C for 45

min. Cells were harvested, frozen in liquid N_2 and lysed by blending in lysis buffer (50 mM HEPES pH 7.4, 150 mM NaCl, 0.1% NP-40 plus phosphatase and protease inhibitors). Lysates were spun at 40,000 rpm for 1 h at 4°C and the supernatant incubated with Flag antibody-coupled magnetic beads for 19 h at 4°C. Beads were washed three times in lysis buffer containing 300 mM NaCl. Bound protein was eluted in 1 M arginine-HCl (pH 3.5) at 4°C for 2 h, frozen in liquid N_2 and stored at −80 °C.

Eluted fractions were diluted to 8 M urea in 100 mM Tris (hydroxyethylamine), pH 8.4, for denaturation and reduction of proteins with 5 mM Tris (2-carboxyethyl) phosphine for 30 min. Cysteine residues were acetylated with 10 mM iodoacetamide for 15 min in the dark. The sample was then diluted to 2 M urea with 100 mM Tris (hydroxyethylamine), pH 8.4, and 1 mM $CaCl_2$, and 0.5 μg trypsin were added and incubated for 4 h at 37°C. The peptide sample was acidified to 5% formic acid and spun at $18,000 \times g$.

Tryptic phosphopeptides were analyzed by Multi-dimensional Protein Identification Technology (MudPIT) as previously described[51], with the following modifications. 3-step MudPIT was performed where each step corresponds to 0, 25, and 100% buffer C (500 mM ammonium acetate) being run for 5 min at the beginning of a 2 h reverse phase gradient. Precursor scanning in the Orbitrap XL was performed from 400 to 2000 m/z with the following settings: 5×10^5 target ions, 50 ms maximum ion injection time, and 1 microscan. Data-dependent acquisitions of MS/MS spectra with the LTQ on the Orbitrap XL were performed with the following settings: MS/MS on the 8 most intense ions per precursor scan, 30K automatic gain control target ions, 100 ms maximum injection time, and 1 microscan. Multistage activation (MSA) fragmentation was performed at 35% normalized collision energy on the precursor and then on the expected neutral loss ions with reduced m/z's of 32.70 (+3 ions), 49.00 (+2), and 98.00 (+1). Dynamic exclusion settings were as follows: repeat count, 1; repeat duration, 30 s; exclusion list size, 500; and exclusion duration, 60 s. Protein and phosphopeptide identification and phosphorylation analysis were done with Integrated Proteomics Pipeline (IP2, www.integratedproteomics.com). Tandem mass spectra were extracted to MS2 files from raw files using RawExtract 1.9.9 and were searched against the SGD *S. cerevisiae* protein database (1/5/2010) with reversed sequences using ProLuCID with the multistage search option[52]. The search space included all fully- and half-tryptic peptide candidates. The MSA search option in ProLuCID models both precursor fragment ions and neutral loss fragment ions in the XCorr calculation. Fragment ions from the phosphopeptide precursor were modeled with a mass increase of 79.9663 Da to the original peptide sequence for each phosphate present. The neutral loss fragment ions were modeled with a mass shift of −18.0106 from the loss of water from the original peptide sequence after the neutral loss of phosphate in the first activation step of MSA. Carbamidomethylation (+57.02146) of cysteine was considered as a static modification; phosphorylation (+79.9663) on serine, threonine, and tyrosine were considered as variable modifications. Peptide candidates were filtered to 0.1% FDR using DTASelect[53,54].

Fig. 2a is the MSA CID fragmentation spectrum of the doubly phosphorylated peptide STGTIpTLNpSSPLKK. From initial unsuccessful attempts with CID fragmentation of the precursor ion only, we found that MSA (ref. 55) provided an adequate balance of sequence-specific and phosphorylation site-specific fragment ions for identification of

phosphorylation sites on this complex phosphopeptide. The six potential sites of phosphorylation complicated phosphate localization and created multiple phosphate neutral losses (−98 Da) and water losses (−18 Da) during fragmentation. Fortunately, an adequate number of sequence-specific ions for peptide identification were identified with MSA, many with water losses. Additionally, phosphate molecules were detected intact on fragment ions y_9 and y_{10}, yet not on y_5, unambiguously indicating that Thr94 and Ser98 were phosphorylated. Further, preferential cleavage N-terminal of the two proline residues within the sequence due to the proline effect[56] conveniently aided generation of both sequence- and phosphorylation site-specific ions. Supplementary Fig. 1 provides additional support of both dual Thr94 and Ser98 phosphorylation and singly phosphorylated peptides. Due to co-migration and co-fragmentation of phosphopeptides with LC-MS/MS (ref. 57), we also found site-specific fragment ions for individual phosphorylation at Ser89, Thr90, and Ser99, as indicated in Fig. 2b and Supplementary Fig. 1. Ultimately, either the lower abundance of these phosphopeptides, or proline effect-favorable fragmentation pathways, may have hindered the identification of other phosphorylation sites.

Kinase Assays

Clb2-Cdk1 and Mck1 were purified from yeast cells overexpressing TAP-tagged versions, as described[58]. Cdc7–Dbf4-Flag from yeast cells was kindly provided by the lab of Stephen Bell. Cdk1 was incubated at room temperature with 1 μM GST-Eco1 (purified from bacteria) in a 30 μl reaction containing 25 mM HEPES (pH 8.0), 15 mM NaCl, 1 mM $MgCl_2$, 1 mM DTT, 4 μCi γ-^{32}P-ATP (3000 Ci/mmol), and 100 μM unlabeled ATP. Reaction products were analyzed by SDS-PAGE and autoradiography.

Peptide kinase assays were performed as above, in duplicate, using peptides synthesized by NeoBioSciences (Cambridge, MA) in 15 μl total volume with 10 μM peptide (Cdk1 reactions), 33 μM peptide (Cdc7 reactions), or 5 μM peptide (Mck1 reactions) for 45 min (Cdk1), 30 min (Mck1), or 15 min (Cdc7). Reactions were stopped by spotting on P81 phosphocellulose paper (Whatman), washed five times for 5 min each in 75 mM phosphoric acid, followed by a single 5 min wash in acetone. Peptides included an extra C-terminal lysine to enhance peptide binding to phosphocellulose. Air-dried papers were counted on a scintillation counter (Beckman Coulter LS 6500). Counts were converted to moles of total phosphate using a standard curve.

Fluorescence Anisotropy

Phosphopeptides containing the Eco1 degron sequence plus a C-terminal tyrosine and cysteine to provide a means of absorbance detection and to conjugate a FITC fluorophore were synthesized by NeoBioSciences and purified by HPLC. Lyophilized peptides were resuspended in 1 ml 50 mM Tris-HCl (pH 7.4) to a final concentration of 1–3 mM and stored at −20°C. His_6-Cdc4-LP6DelA GST-Skp1 was purified from bacteria as described[7]. Equilibrium binding of FITC-peptides to Cdc4 was measured by fluorescence polarization at room temperature in 96-well plates in triplicate (except the two highest Cdc4 concentrations, done in duplicate) in 40 μl 50 mM Tris-HCl (pH 7.4), 100 mM NaCl, 5 mM β-ME, 5% glycerol, 0.1 mg/ml BSA, plus 5 nM peptide and varying concentrations of Cdc4-Skp1. An LJL Biosystems Analyst AD plate reader was used with 495 nM excitation and 525 nM

emission wavelengths, 10 reads per well, 100 ms integration time, and a z-height of 0.5 mm. Background fluorescence was normalized to a reaction lacking peptide. Data were analyzed using Prism software.

Damage-Induced Cohesion Assay

P_{SCC1}-scc1(TEV268)-HA_3:hphNT1:P_{SCC1}:natNT2:P_{MET25}-GFP-SCC1 trp1::TRP1:P_{GAL1}-NLS-myc_6-TEV-NLS_2 ura3::$lacO_{256}$:LEU2 his3::P_{CUP1-1}-GFP-LacI:HIS3 cells were grown overnight in YEP media containing 2% raffinose, then arrested in mitosis with nocodazole for 3 h at 30°C. Cultures were transferred to synthetic media lacking methionine (to induce expression of wild-type Scc1 or Scc1 K84R K210R) and containing nocodazole plus either 333 μg/ml zeocin (first experiment) or 2 μM 4-NQO (second experiment) for 1.5 h to establish cohesion or not. Galactose was then added to 2% for 2 h to express TEV protease and cleave the cohesion established during S phase. 100 μM $CuSO_4$ was added for the last 30 min to fully induce GFP-LacI expression, followed by fixation of cells with 4% paraformaldehyde for 8 min. Cells were washed, resuspended in dibasic sodium phosphate buffer, affixed to concanavalin A-coated slides, and visualized by epifluorescence microscopy.

Supplementary Material

Refer to Web version on PubMed Central for supplementary material.

Acknowledgments

References

1. Holt LJ, et al. Global analysis of Cdk1 substrate phosphorylation sites provides insights into evolution. Science. 2009; 325:1682–6. [PubMed: 19779198]

2. Ubersax JA, et al. Targets of the cyclin-dependent kinase Cdk1. Nature. 2003; 425:859–64. [PubMed: 14574415]

3. Petroski MD, Deshaies RJ. Function and regulation of cullin-RING ubiquitin ligases. Nat Rev Mol Cell Biol. 2005; 6:9–20. [PubMed: 15688063]

4. Welcker M, Clurman BE. FBW7 ubiquitin ligase: a tumour suppressor at the crossroads of cell division, growth and differentiation. Nat Rev Cancer. 2008; 8:83–93. [PubMed: 18094723]

5. Nash P, et al. Multisite phosphorylation of a CDK inhibitor sets a threshold for the onset of DNA replication. Nature. 2001; 414:514–21. [PubMed: 11734846]

6. Hao B, Oehlmann S, Sowa ME, Harper JW, Pavletich NP. Structure of a Fbw7-Skp1-Cyclin E Complex: Multisite-Phosphorylated Substrate Recognition by SCF Ubiquitin Ligases. Mol Cell. 2007; 26:131–43. [PubMed: 17434132]

7. Bao MZ, Shock TR, Madhani HD. Multisite phosphorylation of the Saccharomyces cerevisiae filamentous growth regulator Tec1 is required for its recognition by the E3 ubiquitin ligase adaptor Cdc4 and its subsequent destruction in vivo. Eukaryot Cell. 2010; 9:31–6. [PubMed: 19897738]

8. Welcker M, Clurman BE. Fbw7/hCDC4 dimerization regulates its substrate interactions. Cell Div. 2007; 2:7. [PubMed: 17298674]

9. Tang X, et al. Suprafacial orientation of the SCFCdc4 dimer accommodates multiple geometries for substrate ubiquitination. Cell. 2007; 129:1165–76. [PubMed: 17574027]

10. Lyons NA, Morgan DO. Cdk1-dependent destruction of Eco1 prevents cohesion establishment after S phase. Mol Cell. 2011; 42:378–89. [PubMed: 21549314]

11. Rolef Ben-Shahar T, et al. Eco1-dependent cohesin acetylation during establishment of sister chromatid cohesion. Science. 2008; 321:563–6. [PubMed: 18653893]

12. Rowland BD, et al. Building sister chromatid cohesion: smc3 acetylation counteracts an antiestablishment activity. Mol Cell. 2009; 33:763–74. [PubMed: 19328069]

13. Sutani T, Kawaguchi T, Kanno R, Itoh T, Shirahige K. Budding yeast Wpl1(Rad61)-Pds5 complex counteracts sister chromatid cohesion-establishing reaction. Curr Biol. 2009; 19:492–7. [PubMed: 19268589]

14. Unal E, et al. A molecular determinant for the establishment of sister chromatid cohesion. Science. 2008; 321:566–9. [PubMed: 18653894]

15. Strom L, et al. Postreplicative formation of cohesion is required for repair and induced by a single DNA break. Science. 2007; 317:242–5. [PubMed: 17626884]

16. Strom L, Lindroos HB, Shirahige K, Sjogren C. Postreplicative recruitment of cohesin to double-strand breaks is required for DNA repair. Mol Cell. 2004; 16:1003–15. [PubMed: 15610742]

17. Unal E, Heidinger-Pauli JM, Koshland D. DNA double-strand breaks trigger genome-wide sister-chromatid cohesion through Eco1 (Ctf7). Science. 2007; 317:245–8. [PubMed: 17626885]

18. Sjogren C, Nasmyth K. Sister chromatid cohesion is required for postreplicative double-strand break repair in Saccharomyces cerevisiae. Curr Biol. 2001; 11:991–5. [PubMed: 11448778]

19. Heidinger-Pauli JM, Unal E, Guacci V, Koshland D. The kleisin subunit of cohesin dictates damage-induced cohesion. Mol Cell. 2008; 31:47–56. [PubMed: 18614046]

20. Heidinger-Pauli JM, Unal E, Koshland D. Distinct targets of the Eco1 acetyltransferase modulate cohesion in S phase and in response to DNA damage. Mol Cell. 2009; 34:311–21. [PubMed: 19450529]

21. Kinoshita E, Kinoshita-Kikuta E, Takiyama K, Koike T. Phosphate-binding tag, a new tool to visualize phosphorylated proteins. Mol Cell Proteomics. 2006; 5:749–57. [PubMed: 16340016]

22. Cho WH, Lee YJ, Kong SI, Hurwitz J, Lee JK. CDC7 kinase phosphorylates serine residues adjacent to acidic amino acids in the minichromosome maintenance 2 protein. Proc Natl Acad Sci U S A. 2006; 103:11521–6. [PubMed: 16864800]

23. Masai H, et al. Human Cdc7-related kinase complex. In vitro phosphorylation of MCM by concerted actions of Cdks and Cdc7 and that of a criticial threonine residue of Cdc7 bY Cdks. J Biol Chem. 2000; 275:29042–52. [PubMed: 10846177]

24. Mok J, et al. Deciphering protein kinase specificity through large-scale analysis of yeast phosphorylation site motifs. Sci Signal. 2010; 3:ra12. [PubMed: 20159853]

25. Randell JC, et al. Mec1 is one of multiple kinases that prime the Mcm2-7 helicase for phosphorylation by Cdc7. Mol Cell. 2010; 40:353–63. [PubMed: 21070963]

26. Oshiro G, Owens JC, Shellman Y, Sclafani RA, Li JJ. Cell cycle control of Cdc7p kinase activity through regulation of Dbf4p stability. Mol Cell Biol. 1999; 19:4888–96. [PubMed: 10373538]

27. Sullivan M, Holt L, Morgan DO. Cyclin-specific control of ribosomal DNA segregation. Mol Cell Biol. 2008; 28:5328–36. [PubMed: 18591250]

28. Labib K. How do Cdc7 and cyclin-dependent kinases trigger the initiation of chromosome replication in eukaryotic cells? Genes Dev. 2010; 24:1208–19. [PubMed: 20551170]

29. Marston AL. Meiosis: DDK is not just for replication. Curr Biol. 2009; 19:R74–6. [PubMed: 19174144]

30. Jackson AL, Pahl PM, Harrison K, Rosamond J, Sclafani RA. Cell cycle regulation of the yeast Cdc7 protein kinase by association with the Dbf4 protein. Mol Cell Biol. 1993; 13:2899–908. [PubMed: 8474449]

31. Doble BW, Woodgett JR. GSK-3: tricks of the trade for a multi-tasking kinase. J Cell Sci. 2003; 116:1175–86. [PubMed: 12615961]

32. Fiol CJ, Mahrenholz AM, Wang Y, Roeske RW, Roach PJ. Formation of protein kinase recognition sites by covalent modification of the substrate. Molecular mechanism for the synergistic action of casein kinase II and glycogen synthase kinase 3. J Biol Chem. 1987; 262:14042–8. [PubMed: 2820993]

33. Xu C, Kim NG, Gumbiner BM. Regulation of protein stability by GSK3 mediated phosphorylation. Cell Cycle. 2009; 8:4032–9. [PubMed: 19923896]

34. Kassir Y, Rubin-Bejerano I, Mandel-Gutfreund Y. The Saccharomyces cerevisiae GSK-3 beta homologs. Curr Drug Targets. 2006; 7:1455–65. [PubMed: 17100585]

35. Mizunuma M, Hirata D, Miyaoka R, Miyakawa T. GSK-3 kinase Mck1 and calcineurin coordinately mediate Hsl1 down-regulation by Ca2+ in budding yeast. EMBO J. 2001; 20:1074–85. [PubMed: 11230131]

36. Kishi T, Ikeda A, Nagao R, Koyama N. The SCFCdc4 ubiquitin ligase regulates calcineurin signaling through degradation of phosphorylated Rcn1, an inhibitor of calcineurin. Proc Natl Acad Sci U S A. 2007; 104:17418–23. [PubMed: 17954914]

37. Ikui AE, Rossio V, Schroeder L, Yoshida S. A yeast GSK-3 kinase Mck1 promotes Cdc6 degradation to inhibit DNA re-replication. PLoS Genetics. 2012 in press.

38. Koivomagi M, et al. Cascades of multisite phosphorylation control Sic1 destruction at the onset of S phase. Nature. 2011; 480:128–31. [PubMed: 21993622]

39. Tang X, et al. Composite low affinity interactions dictate recognition of the cyclin-dependent kinase inhibitor Sic1 by the SCFCdc4 ubiquitin ligase. Proc Natl Acad Sci U S A. 2012; 109:3287–92. [PubMed: 22328159]

40. Liu Q, et al. SCFCdc4 enables mating type switching in yeast by cyclin-dependent kinase-mediated elimination of the Ash1 transcriptional repressor. Mol Cell Biol. 2011; 31:584–98. [PubMed: 21098119]

41. Kihara M, et al. Characterization of the yeast Cdc7p/Dbf4p complex purified from insect cells. Its protein kinase activity is regulated by Rad53p. J Biol Chem. 2000; 275:35051–62. [PubMed: 10964916]

42. Weinreich M, Stillman B. Cdc7p-Dbf4p kinase binds to chromatin during S phase and is regulated by both the APC and the RAD53 checkpoint pathway. EMBO J. 1999; 18:5334–46. [PubMed: 10508166]

43. Lei M, et al. Mcm2 is a target of regulation by Cdc7-Dbf4 during the initiation of DNA synthesis. Genes Dev. 1997; 11:3365–74. [PubMed: 9407029]

44. Gabrielse C, et al. A Dbf4p BRCA1 C-terminal-like domain required for the response to replication fork arrest in budding yeast. Genetics. 2006; 173:541–55. [PubMed: 16547092]

45. Takeda T, et al. Regulation of initiation of S phase, replication checkpoint signaling, and maintenance of mitotic chromosome structures during S phase by Hsk1 kinase in the fission yeast. Mol Biol Cell. 2001; 12:1257–74. [PubMed: 11359920]

46. Lopez-Mosqueda J, et al. Damage-induced phosphorylation of Sld3 is important to block late origin firing. Nature. 2010; 467:479–83. [PubMed: 20865002]

47. Zegerman P, Diffley JF. Checkpoint-dependent inhibition of DNA replication initiation by Sld3 and Dbf4 phosphorylation. Nature. 2010; 467:474–8. [PubMed: 20835227]

48. Mantiero D, Mackenzie A, Donaldson A, Zegerman P. Limiting replication initiation factors execute the temporal programme of origin firing in budding yeast. EMBO J. 2011; 30:4805–14. [PubMed: 22081107]

49. Tanaka S, Nakato R, Katou Y, Shirahige K, Araki H. Origin association of Sld3, Sld7, and Cdc45 proteins is a key step for determination of origin-firing timing. Curr Biol. 2011; 21:2055–63. [PubMed: 22169533]

50. Longtine MS, et al. Additional modules for versatile and economical PCR-based gene deletion and modification in *Saccharomyces cerevisiae*. Yeast. 1998; 14:953–961. [PubMed: 9717241]

51. Wolters DA, Washburn MP, Yates JR 3rd. An automated multidimensional protein identification technology for shotgun proteomics. Anal Chem. 2001; 73:5683–90. [PubMed: 11774908]

52. Fonslow BR, et al. Single-step inline hydroxyapatite enrichment facilitates identification and quantitation of phosphopeptides from mass-limited proteomes with MudPIT. J Proteome Res. 2012; 11:2697–709. [PubMed: 22509746]

53. Cociorva D, DLT, Yates JR. Validation of tandem mass spectrometry database search results using DTASelect. Curr Protoc Bioinformatics. 2007; Chapter 13(Unit 13):4. [PubMed: 18428785]

54. Tabb DL, McDonald WH, Yates JR 3rd. DTASelect and Contrast: tools for assembling and comparing protein identifications from shotgun proteomics. J Proteome Res. 2002; 1:21–6. [PubMed: 12643522]

55. Schroeder MJ, Shabanowitz J, Schwartz JC, Hunt DF, Coon JJ. A neutral loss activation method for improved phosphopeptide sequence analysis by quadrupole ion trap mass spectrometry. Anal Chem. 2004; 76:3590–8. [PubMed: 15228329]

56. Breci LA, Tabb DL, Yates JR 3rd, Wysocki VH. Cleavage N-terminal to proline: analysis of a database of peptide tandem mass spectra. Anal Chem. 2003; 75:1963–71. [PubMed: 12720328]

57. Courcelles M, Bridon G, Lemieux S, Thibault P. Occurrence and detection of phosphopeptide isomers in large-scale phosphoproteomics experiments. J Proteome Res. 2012; 11:3753–65. [PubMed: 22668510]

58. Loog M, Morgan DO. Cyclin specificity in the phosphorylation of cyclin-dependent kinase substrates. Nature. 2005; 434:104–108. [PubMed: 15744308]
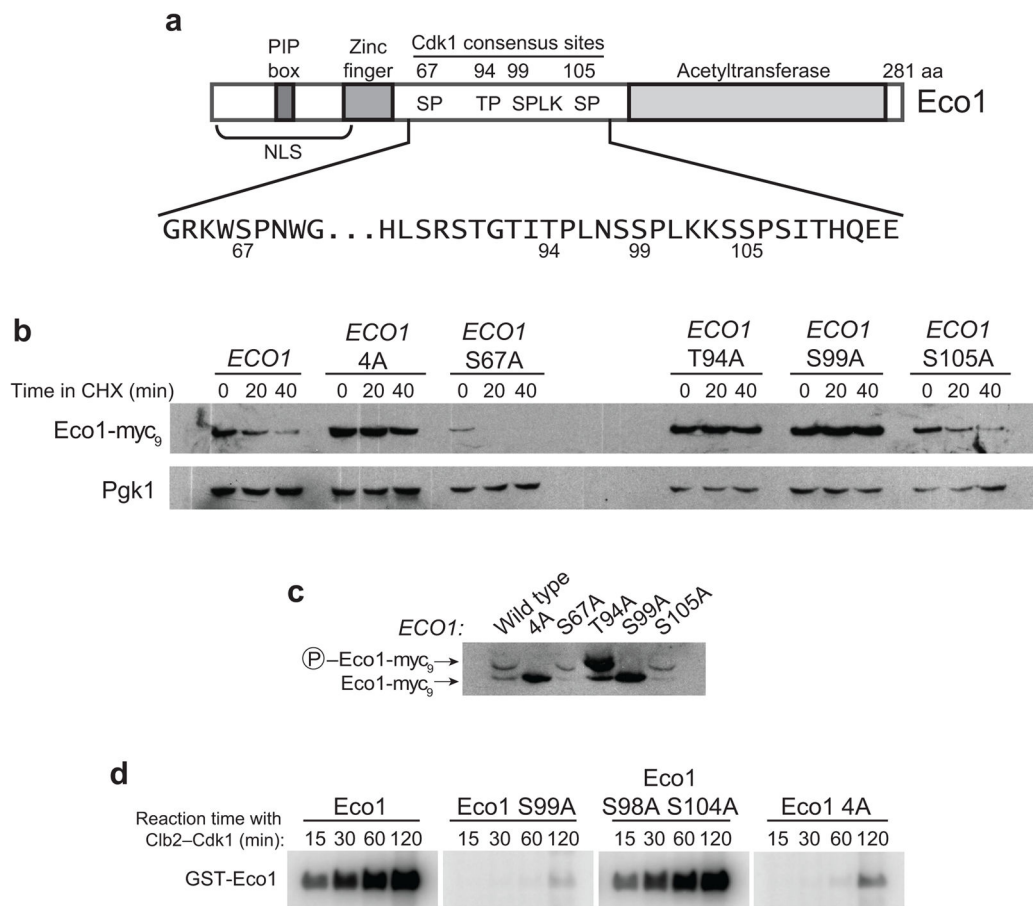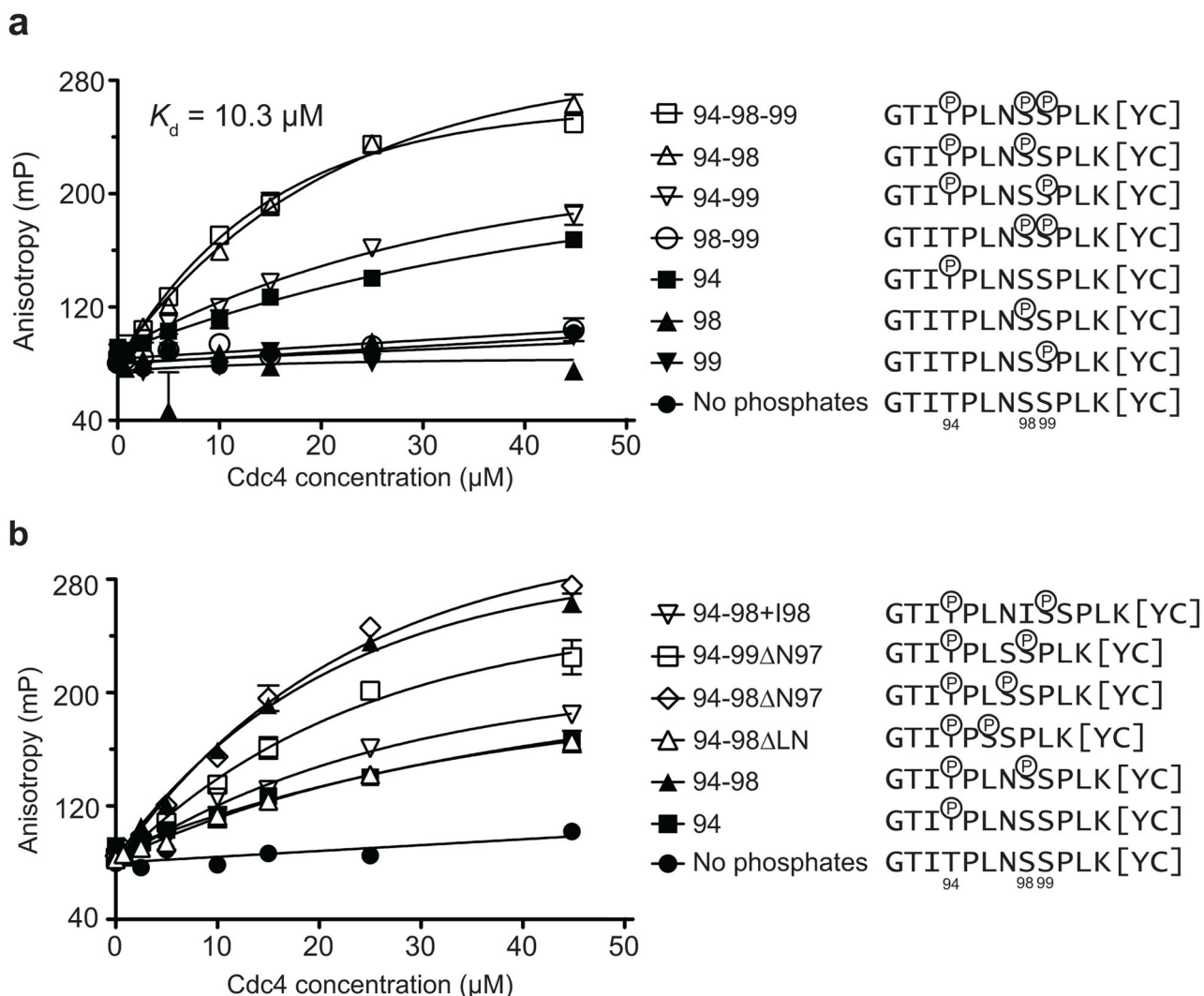
Figure 1.
Analysis of the contribution of individual Cdk1 sites to Eco1 degradation. (**a**) Schematic of Eco1 domain structure highlighting the four Cdk1 consensus sites. PIP, PCNA-interacting protein domain; NLS, nuclear localization sequence. (**b**) Western blot for measurement of Eco1 stability in mitotic yeast cells. The indicated strains were arrested in mitosis with nocodazole and then treated with cycloheximide (CHX). Cell lysates were prepared for analysis by SDS-PAGE and western blotting, using Pgk1 as a loading control. The Eco1 4A mutant lacks all four Cdk1 consensus sites. (**c**) Western blot for analysis of phosphate-dependent Eco1 gel mobility shift. Lysates from the zero time points in panel **b** were analyzed on an SDS-PAGE gel containing Phos-tag reagent to slow the mobility of phosphorylated proteins. (**d**) Measurement of Cdk1 kinase activity toward Eco1 *in vitro*. Recombinant GST-Eco1 was incubated with purified Clb2–Cdk1 and radiolabeled ATP for the indicated times, and analyzed by SDS-PAGE and autoradiography.
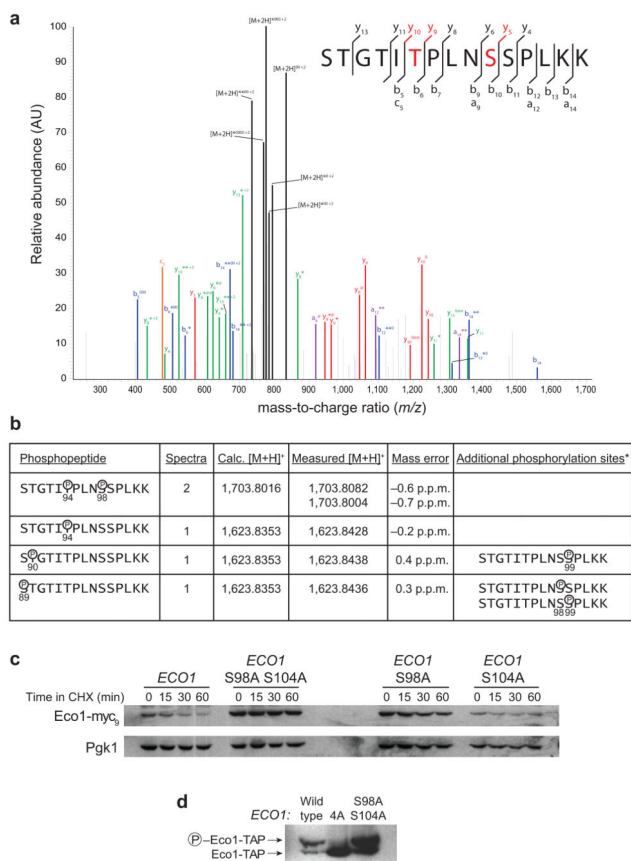
Figure 2.
Mass spectrometry reveals non-Cdk1 phosphorylation of Eco1. (**a**) Mass spectrum for a representative Eco1 phosphopeptide. Eco1-Flag$_3$His$_6$ was purified from yeast cultures in which *CDC4* expression was repressed, and digested with trypsin and subjected to tandem mass spectrometry. Sequence-informative fragmentation ions are summarized on the peptide sequence and annotated in blue (b-ions), green (y-ions), orange (c-ions), and purple (a-ions); phosphorylation site-specific ions are in red. Phosphate neutral loss (*), water loss (^{0}), and ammonia loss ($^@$) are annotated on b- and y-ions on the spectra. Different combinations of phosphate neutral loss and water and ammonia loss from precursor ions are annotated in black as [M+2H]$^{+2}$. (**b**) Phosphopeptides identified by tandem mass spectrometry in order of confidence. The number of spectra identified for each phosphopeptide is listed, along with the calculated (Calc.) and measured monoisotopic masses of the phosphopeptides ([M+H]$^+$) and the accuracy of the mass measurements in parts per million. *A subset of the fragment ions from these spectra showed evidence for phosphates on the indicated alternative residues. See Supplementary Fig. 1 for all annotated spectra. (**c**) Western blot for measurement of Eco1 stability in mitotic yeast cells, as in Fig. 1b. (**d**) Western blot for analysis of phosphate-dependent Eco1 mobility shift on a Phos-Tag gel, as in Fig. 1c.
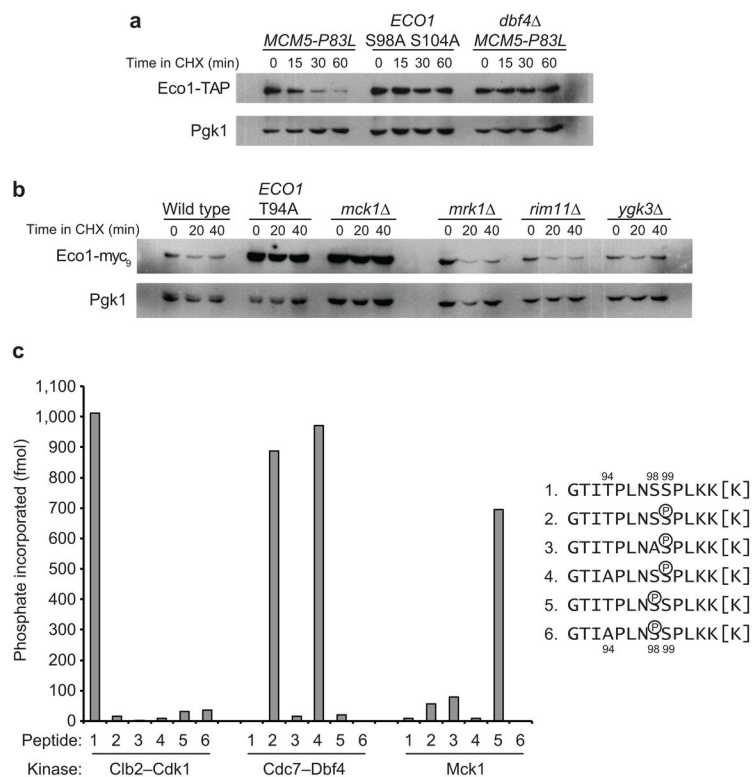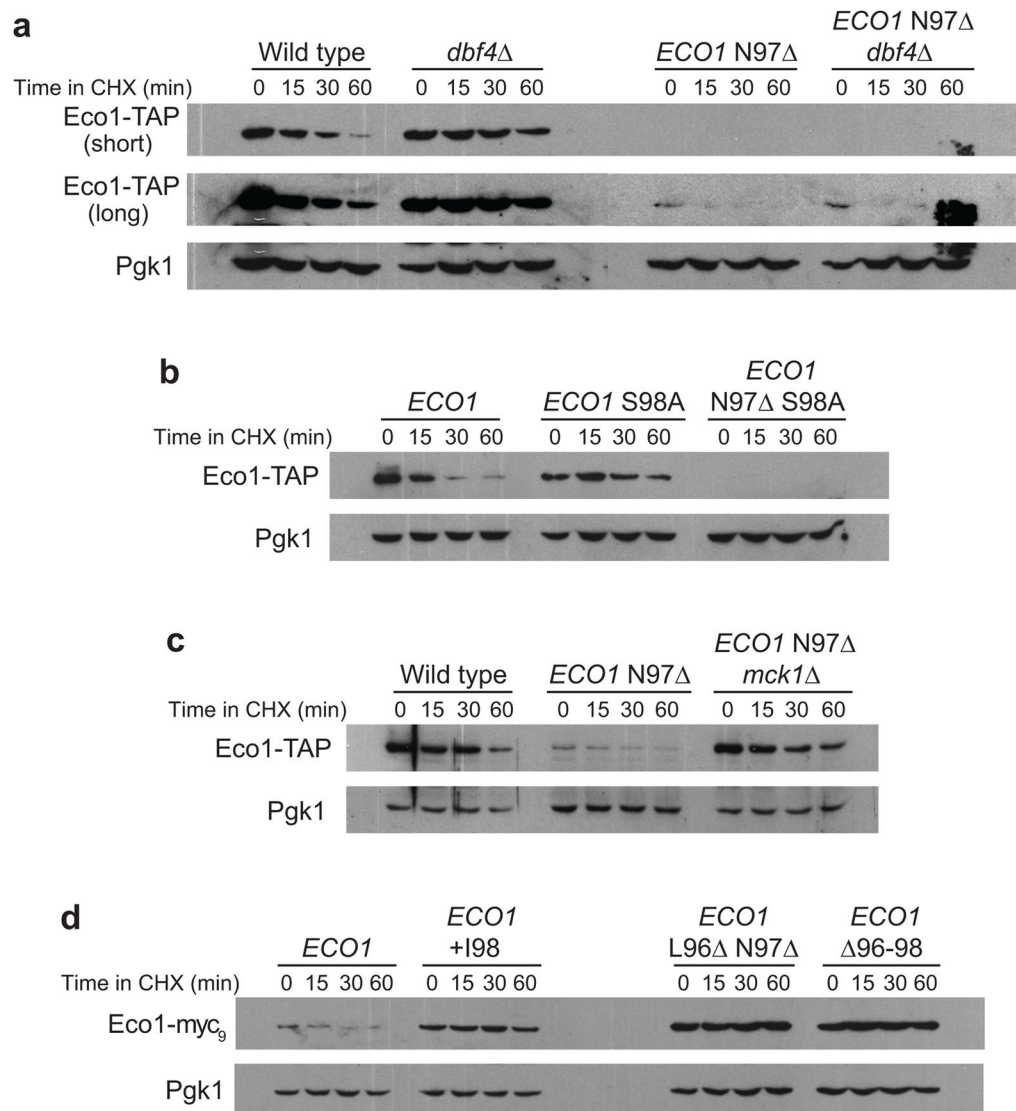
Figure 3.
Cdc7–Dbf4 and Mck1 are necessary for full degradation of Eco1 and phosphorylate Eco1 peptides *in vitro*. (**a**) Western blots to measure Eco1 stability in mitotic yeast cells, as in Fig. 1b. (**b**) Western blots to measure Eco1 stability in mitotic yeast cells lacking each of the four GSK-3 family members, as in Fig. 1b. (**c**) Determination of kinase activities toward phosphopeptides in vitro. Synthetic peptides based on residues 91–103 of Eco1 (plus an additional C-terminal lysine; sequences at right) were incubated with the indicated purified kinase and γ-^{32}P-ATP. For each kinase, phosphate incorporation was normalized to a background control reaction containing no peptide. Values are means from at least two independent reactions.
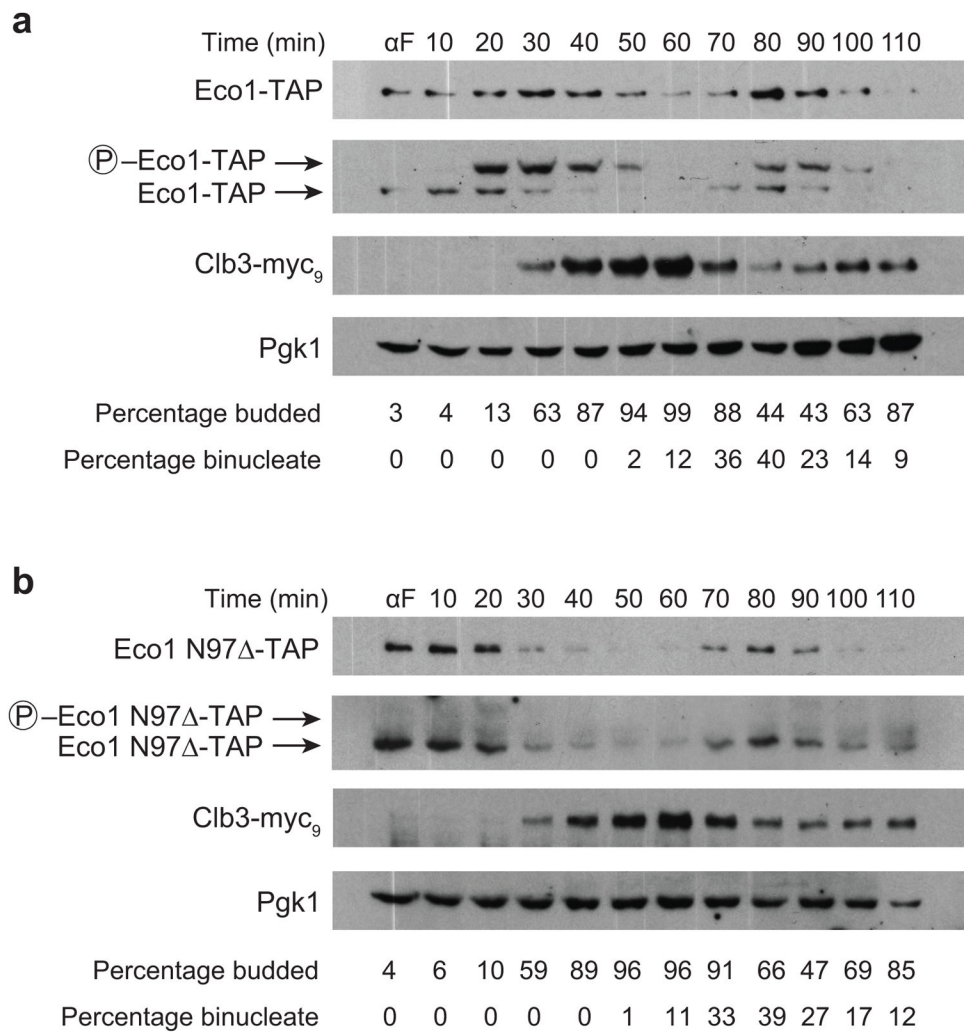
Figure 4.
Cdc4 binding depends on precise spacing of phosphorylation sites in Eco1. (**a,b**) Fluorescence anisotropy measurements of peptide binding to Cdc4. FITC-conjugated phosphopeptides derived from Eco1 were incubated with increasing concentrations of Cdc4–Skp1 complex *in vitro*, and the polarization of the fluorescent peptides was used to measure binding. Values are means from two or three experiments (error bars indicate S.E.M.). Data for the "no phosphate", "94", and "94-98" peptides in panel **b** are reproduced from panel **a**. In the peptide sequences shown at right, the residues in brackets are for conjugation and purification purposes and are not part of the Eco1 sequence.

Figure 5.
Correct phosphate spacing is essential for Eco1 turnover in the cell. (**a–d**) Western blots to monitor Eco1 stability in mitotic yeast cells, as in Fig. 1b. The *dbf4* strains used in panel **a** contain the *MCM5-P83L* suppressor mutation. In panel **a**, two different exposures of the Eco1 western blot are provided to illustrate the low level of Eco1 N97 protein.

Figure 6.
DDK activity limits Eco1 degradation to late S phase. (**a, b**) Western blots to monitor Eco1 levels during the cell cycle. *ECO1-TAP* (**a**) or *ECO1-N97 -TAP* cells (**b**) were arrested in G1 with α-factor (αF) and then released. At the indicated times, samples were harvested for analysis by western blotting and microscopy. To visualize phosphorylated forms of Eco1, samples were run on separate SDS-PAGE gels containing Phos-tag reagent.
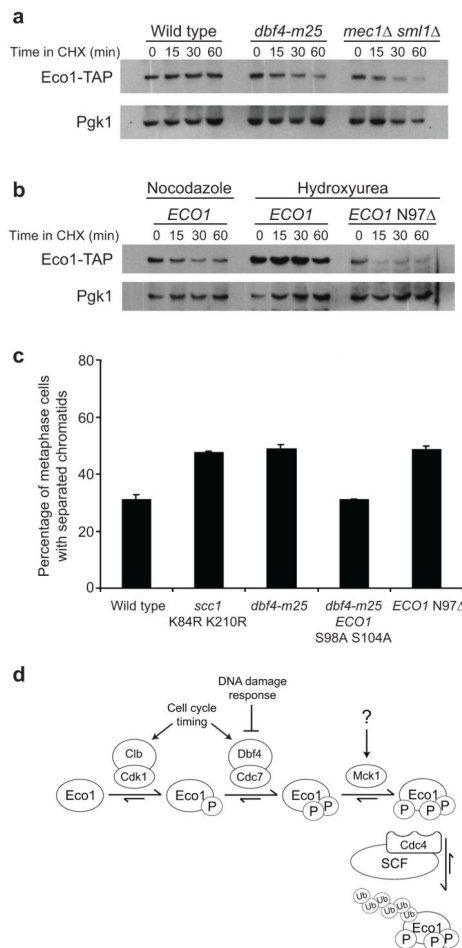
Figure 7.
DDK inhibition allows damage-induced cohesion establishment. (**a**) Western blots to measure Eco1 stability during a DNA damage response. Cells were arrested in nocodazole plus hydroxyurea, followed by addition of cycloheximide (CHX). Cell lysates were analyzed by western blotting, using Pgk1 as a loading control. The *sml1* deletion is required for viability of *mec1* cells. (**b**) Western blot monitoring Eco1 stability. Cells were arrested in mitosis with either nocodazole or hydroxyurea, followed by treatment with cycloheximide (CHX). Cell lysates were analyzed by western blotting, using Pgk1 as a loading control. (**c**) Analysis of cohesion establishment following DNA damage. Separation of GFP-tagged sister chromatids was used to measure the establishment of new sister-chromatid cohesion in mitotic cells treated with DNA damaging agents (see Methods for details). At least 200 cells were counted, and an average taken from two biological repeats (error bars represent S.E.M.). The differences between wild type and *scc1* K84R K210R, *dbf4-m25*, and *ECO1* N97 are each statistically significant (P=0.004; standard t-test). (**d**) Model of sequential Eco1 phosphorylation and ubiquitination. Beginning in early S phase, Cdk1 catalyzes phosphorylation of Ser99, which primes Cdc7–Dbf4 to phosphorylate Ser98 in late S phase through mitosis. This primes Mck1 to phosphorylate Thr94 and create a binding site for SCF-Cdc4, leading to ubiquitination and subsequent destruction by the proteasome. The DNA damage response blocks this sequence of events by inhibiting Cdc7–Dbf4. Cdk1 and

Cdc7 activities are determined by cell cycle position, but the regulation of Mck1 is unknown.